Extended Abstract for 2004 AAS/AIAA Space Flight Mechanics Meeting,
Maui, Hawaii, Feb. 8-12, 2004

Proof Mass Dynamic Gravitational Balancing for the Laser Interferometry Space Antenna (LISA)[2]

Dr. Marco B. Quadrelli
M.S. 198-326
Jet Propulsion Laboratory
California Institute of Technology
4800 Oak Grove Drive
Pasadena, CA 91109
marco@grover.jpl.nasa.gov

LISA is a space-borne gravitational wave detector, which is formed by three spacecraft orbiting the Sun and forming the vertices of an equilateral triangle with a side of 5 million km in length. Inside each spacecraft, shown in Figure 1, an optical bench monitors the motion of two separated proof masses, which reflect the laser light from the adjacent spacecraft along the edges of the equilateral triangle, and senses the gravitational wave signal with unprecedented sensitivity.

This paper considers the feasibility of a non-invasive compensation scheme for precise positioning of a massive extended body in free fall using gravitational forces caused by surrounding source masses. A number of control masses (CM) move around the proof mass (PM) so that its position can be accurately compensated when exogenous disturbances are acting on it, and its sensitivity to gravitational waves remains therefore unaffected. Past methods to correct the dynamics of the proof mass have considered active electrostatic or capacitive methods, but the possibility of stray capacitances on the surfaces of the LISA cubical proof mass have prompted the investigation of other alternatives, such as the method presented in this paper.

New results are obtained in this paper for the linearized dynamics and stability of gravitationally interacting bodies. We initially assume that all masses are in free space. We can add the spacecraft and orbital base accelerations later. The perturbed displacements of the proof mass and one of the control masses are (Figures 2 and 3):

$$\mathbf{r}_0 = \mathbf{R}_0 + \mathbf{u}_0$$
$$\mathbf{r}_1 = \mathbf{R}_1 + \mathbf{u}_1$$

and the equations of motion of the system are:

[2] This research was performed at the Jet Propulsion Laboratory, California Institute of Technology, under contract with the National Aeronautics and Space Administration.

$$\mathbf{m}_0\ddot{\mathbf{r}}_0 = \mathbf{g}_i^0 + \boldsymbol{\pi}_0$$
$$\mathbf{m}_i\ddot{\mathbf{r}}_i = \mathbf{g}_i + \mathbf{f}_i$$

where π_0 is the perturbation off the geodesic path for m_0 (caused by forces other than gravity, i.e. magnetic forces, electrostatic forces, radiation forces, and others), and $\mathbf{f}_i$ a control force. Assume that initially m_0 is at the zero point of self gravity ($\mathbf{R}_0$ and $\mathbf{d}^i_0$ constants). After linearizing the gravity field, assuming small deviations from initial equilibrium, one obtains:

$$\mathbf{g}_i^0 = +\mu_i \mathbf{d}^i{}_i \left|\mathbf{d}^i{}_i\right|^{-3} \xrightarrow{\textit{linearizing}} \mathbf{g}_i^0 \simeq +\mu_i \Lambda_i \left(\mathbf{u}_i - \mathbf{u}_0\right)$$
$$\mathbf{g}_i = -\mu_i \mathbf{d}^i{}_i \left|\mathbf{d}^i{}_i\right|^{-3}$$

since $\mathbf{d}^i{}_i = \mathbf{d}^i{}_0 + \mathbf{u}_0 - \mathbf{u}_i$, and

$$\Lambda_i = -\frac{2}{(\mathbf{d}^i_0)^3}\mathbf{1}_3 - \frac{3}{(\mathbf{d}^i_0)^5}\left[\mathbf{d}^i_0 \times \mathbf{d}^i_0 \times \mathbf{1}_3\right]$$

One can observe that the matrix Λ_i is not positive definite.

The linearized equations of motion about initial equilibrium of a system of the proof mass PM+6 control masses CM yields:

$$\begin{pmatrix} m_1\mathbf{1}_3 & 0 & 0 & \cdots & 0 \\ 0 & m_2\mathbf{1}_3 & 0 & \vdots & 0 \\ 0 & 0 & m_3\mathbf{1}_3 & \cdots & 0 \\ \vdots & \vdots & \vdots & \vdots & \vdots \\ 0 & 0 & 0 & \cdots & m_N\mathbf{1}_3 \end{pmatrix} \begin{pmatrix} \ddot{\mathbf{u}}_1 \\ \ddot{\mathbf{u}}_2 \\ \ddot{\mathbf{u}}_3 \\ \vdots \\ \ddot{\mathbf{u}}_N \end{pmatrix} + \begin{pmatrix} -\sum_{i\neq 1}\mu_{1i}\Lambda_{11} & \mu_{12}\Lambda_{21} & \mu_{13}\Lambda_{31} & \cdots & \mu_{1N}\Lambda_{N1} \\ \mu_{21}\Lambda_{12} & -\sum_{i\neq 2}\mu_{2i}\Lambda_{12} & \mu_{23}\Lambda_{32} & \cdots & \mu_{2N}\Lambda_{N2} \\ \mu_{31}\Lambda_{13} & \mu_{32}\Lambda_{23} & -\sum_{i\neq 3}\mu_{3i}\Lambda_{13} & \cdots & \mu_{3N}\Lambda_{N3} \\ \vdots & \vdots & \vdots & \vdots & \vdots \\ \mu_{N1}\Lambda_{1N} & \mu_{N2}\Lambda_{2N} & \mu_{N3}\Lambda_{3N} & \cdots & -\sum_{i\neq N}\mu_{Ni}\Lambda_{IN} \end{pmatrix} \begin{pmatrix} \mathbf{u}_1 \\ \mathbf{u}_2 \\ \mathbf{u}_3 \\ \vdots \\ \mathbf{u}_N \end{pmatrix} = \begin{pmatrix} \pi_1 \\ \mathbf{f}_2 \\ \mathbf{f}_3 \\ \vdots \\ \mathbf{f}_N \end{pmatrix}$$

where $\mu_{ij}=Gm_im_j$ and:

$$\Lambda_{ij} = \frac{1}{(\mathbf{d}^0_{ij})^3}\mathbf{1}_3 - \frac{3}{(\mathbf{d}^0_{ij})^5}\left[\mathbf{d}^0_{ij} \times \mathbf{d}^0_{ij} \times \mathbf{1}_3\right]$$

also not positive definite. Therefore dynamic instability is expected. Also, when the point control masses move, the cubical proof mass extended body feels both a resultant force and a resultant torque about its center of mass. The center of gravity of the proof mass is also separated from the center of mass, on account of the mass distribution surrounding it. These details of the mass distribution are very important for this application, as the precision at which the proof mass must be controlled is very high.

Another paper by the author describes the ongoing finite element-based modeling effort being carried out at JPL to determine the gravitational forces and moments, and

force and moment gradients, acting on the LISA proof mass to within the accuracy required for successful operation of the interferometer.

There are several forms that the controller can take. Define by $(\mathbf{u_i}, \mathbf{v_i})$ the displacement and velocity vectors of the control masses (CM), while $(\mathbf{u_0}, \mathbf{v_0})$ are the displacement and velocity vectors of the proof mass (PM), and $(\mathbf{K_i}, \mathbf{D_i})$ are the proportional and derivative gain matrices of the control loop. The proof mass is only actuated via the gravitational interaction. Therefore, one may have that:

1) PM is never actuated, only sensed.
2) Feedback force on CM_i only: $\mathbf{f_i}=-\mathbf{K_i u_i}-\mathbf{D_i v_i}$
3) Feedback force on CM_i and PM: $\mathbf{f_i}=-\mathbf{Ki}(\mathbf{u_i}-\mathbf{u_0})-\mathbf{D_i}\,(\mathbf{v_i}-\mathbf{v_0})$
4) Feedback force on PM only: $\mathbf{f_i}=-\mathbf{K_i u_0}-\mathbf{D_i v_0}$
5) Feedback force plus cancellation terms: $\mathbf{f_i}=-\mathbf{K_i u_i}-\mathbf{D_i v_i}+\mu_i\mathbf{K_i}\,(\mathbf{u_i}-\mathbf{u_0})$

The requirements for PM position control along the non-sensitive axes are: less than 100 micron displacements in the sensitive axis, with 100 nanometer precision in translation, and less than 5 milliradian adjustments, with 50-nanoradian precision in attitude. The basic question is: using a model with point mass CMs and a finite-volume cubical PM, how much linear motion of what combinations and numbers of CMs is required to produce this kind of control of a PM? In this paper we show that the requirements can be met by moving up to 14 control masses (six facing the sides of the proof mass cube, and 8 facing the vertices) around the proof mass (Figure 4), so that the proof mass can be repositioned with a response time of about 15 hours by using the gravitational field of the control masses as the actuation mechanism. A feedback plus feed-forward control scheme is used on the CMs, and a parametric analysis is carried out to determine the sensitivity of the PM response to CM initial positioning and mass, demonstrating effective control of the proof mass within the specified requirements.

Figure 4 depicts the initial configuration of proof mass (large center cube) and 14 control masses (6 facing the sides of the proof mass, 8 facing the corners). Figure 5 shows the displacement (above) and Velocity (below) command profile for the control masses. Figure 6 shows the displacement of the proof mass in microns vs. the simulation time in hours. The proof mass is initially at zero, with a mass of 1.3 Kg, and the residual oscillation is about 90 nm. Figure 7 shows the displacement of the control mass in microns vs. the simulation time in hours. The control mass initially at –0.0554m, with a mass of 1.3 Kg, and the residual oscillation is about 90 nm. Figure 8 shows the effect of control mass size on proof mass stability (vertical axis: displacement of proof mass along X in microns; horizontal axis: simulation time in hours; curves shown: red=3 Kg control mass, magenta=2 Kg control mass, blue=1.3 Kg control mass). Figure 9 shows the effect of control mass distance on proof mass stability (vertical axis: displacement of proof mass along X in microns; horizontal axis: simulation time in hours; curves shown: red= control mass initially located at 4 cm, blue= control mass initially located at 5.544 cm).

Further extensions of this work include: 1) modeling all the control masses as truly extended bodies, 2) an evaluation of the possible sensing and motion estimation possibilities for the proof mass, and 2) optimizing over the number and location of these

control masses to maximize the sensitivity of the proof mass to their motion. The initial results of this paper lay the ground for these further developments.

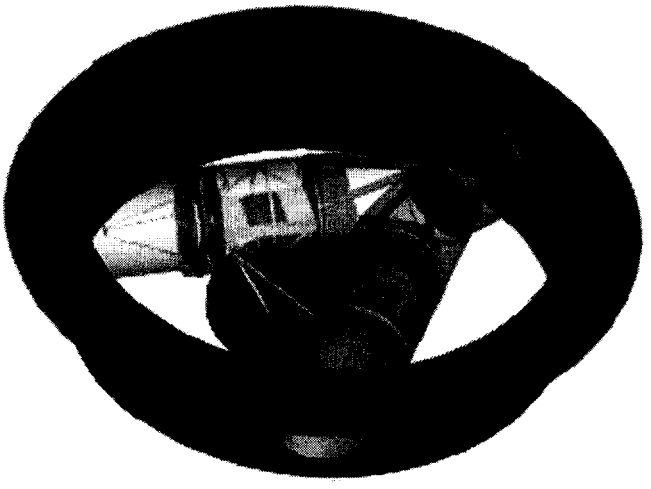

Figure 1. Picture of LISA spacecraft.

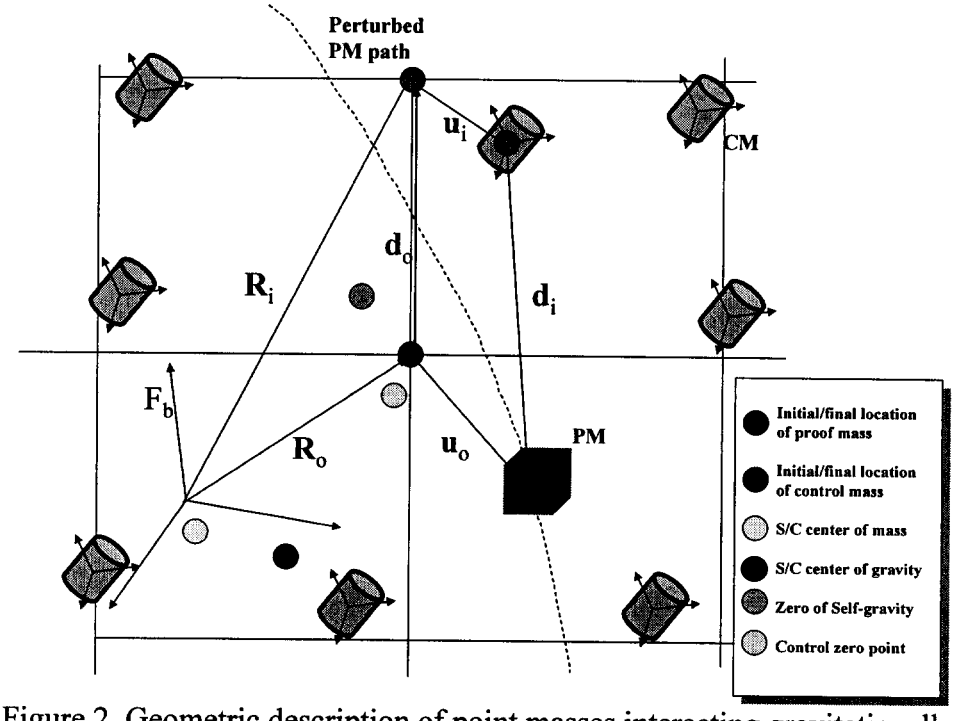

Figure 2. Geometric description of point masses interacting gravitationally.

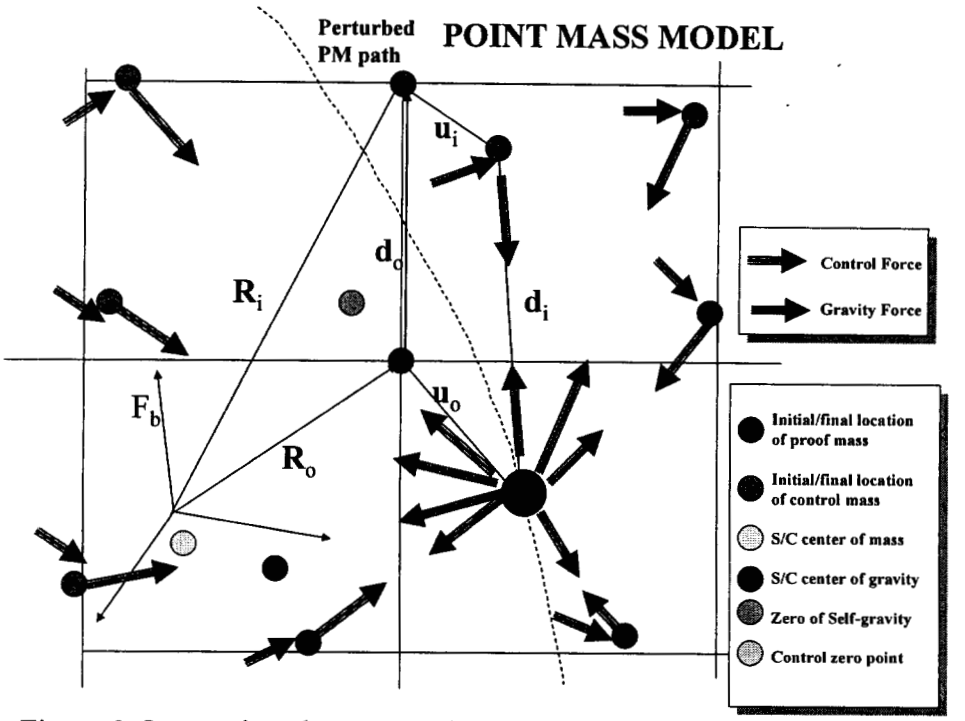

Figure 3. Interactions between point masses in perturbed configuration.

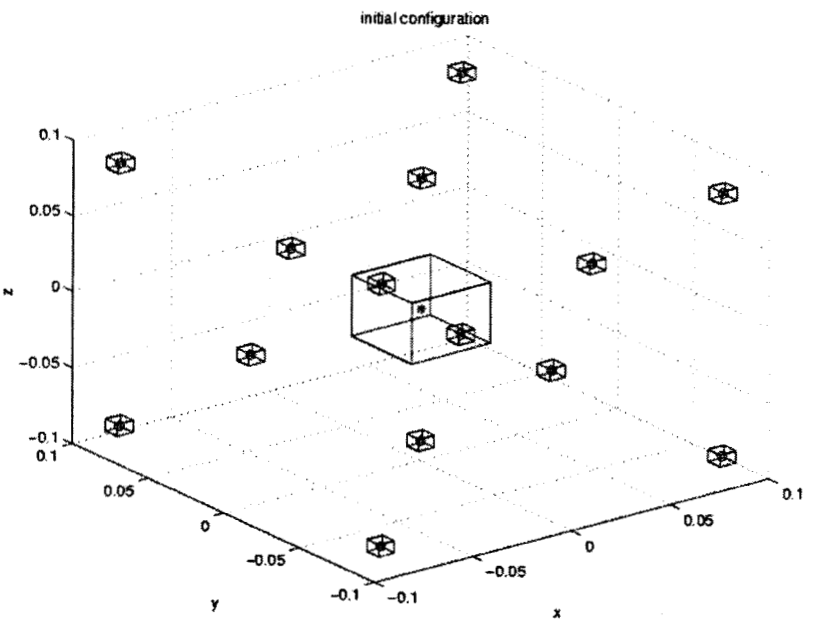

Figure 4. Initial configuration of proof mass (large center cube) and 14 control masses (6 facing the sides of the proof mass, 8 facing the corners).

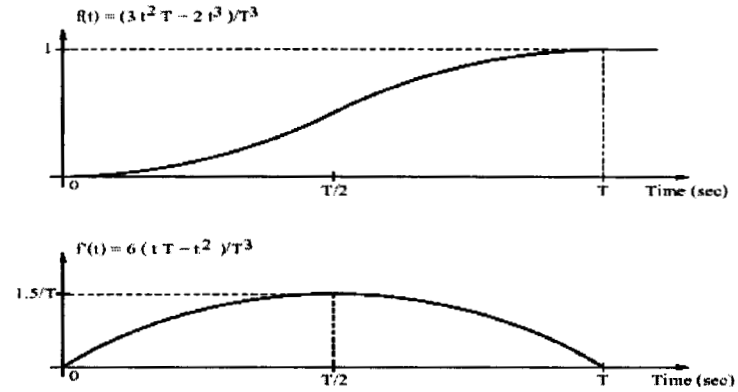

Figure 5. Displacement (above) and Velocity (below) command profile for control masses.

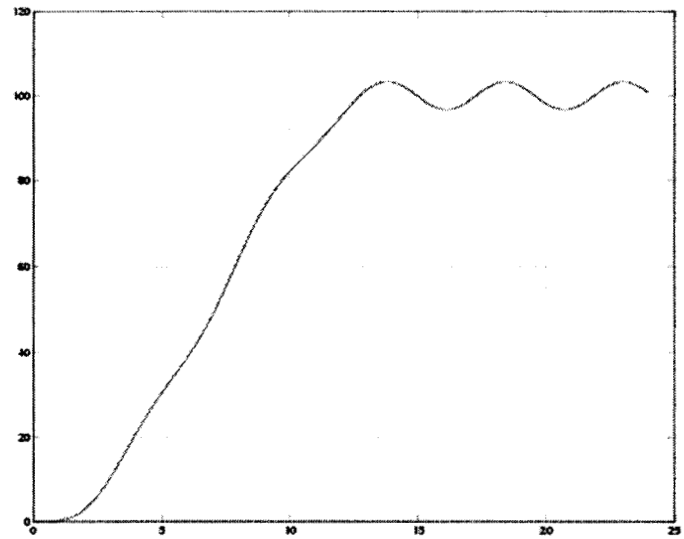

Figure 6. Vertical axis: displacement of proof mass in microns, horizontal axis: simulation time in hours. Proof mass initially at zero, mass=1.3 Kg. Residual oscillation is about 90 nm.

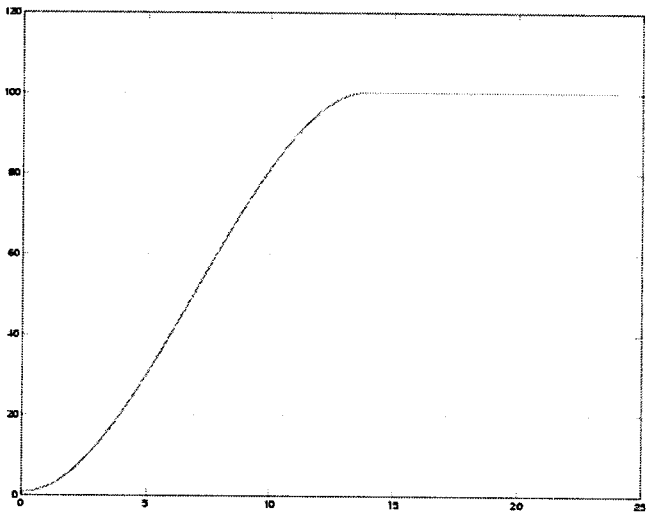

Figure 7. Vertical axis: displacement of control mass in microns, horizontal axis: simulation time in hours. Control mass initially at –0.0554m, mass=1.3 Kg. Residual oscillation is about 90 nm.

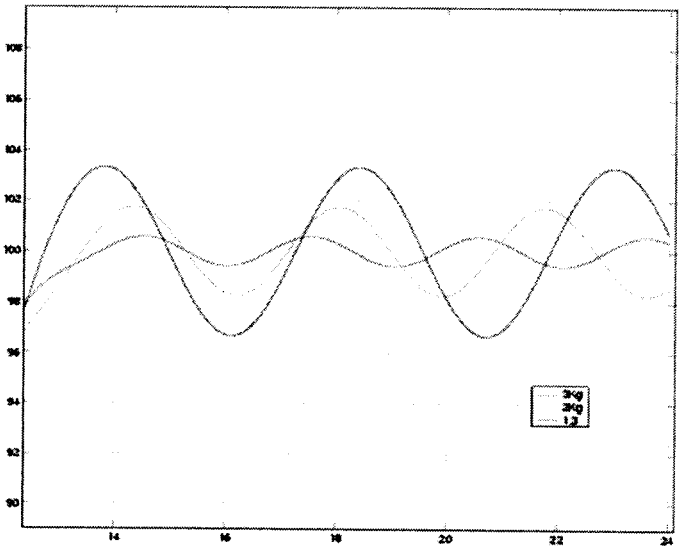

Figure 8. Effect of control mass size on proof mass stability (vertical axis: displacement of proof mass along X in microns; horizontal axis: simulation time in hours; curves shown: red=3 Kg control mass, magenta=2 Kg control mass, blue=1.3 Kg control mass).

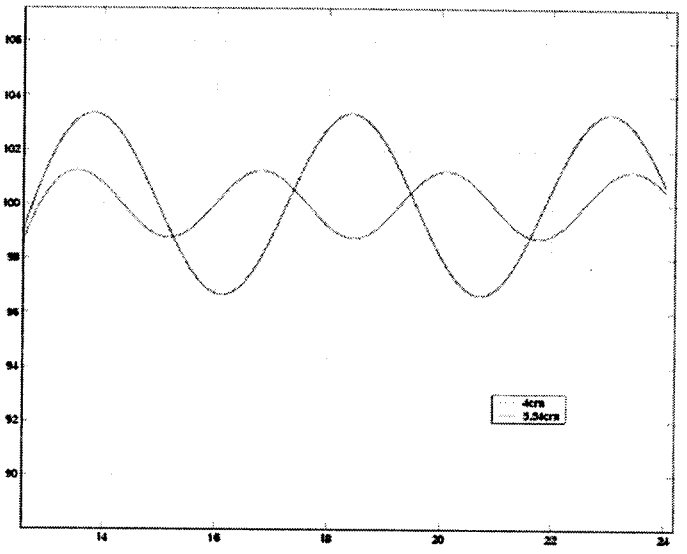

Figure 9. Effect of control mass distance on proof mass stability (vertical axis: displacement of proof mass along X in microns; horizontal axis: simulation time in hours; curves shown: red= control mass initially located at 4 cm, blue= control mass initially located at 5.544 cm).